FEBS Letters 588 (2014) 2874–2880

FEBS Letters

journal homepage: www.FEBSLetters.org

Atomic force microscopy (AFM) imaging suggests that stromal interaction molecule 1 (STIM1) binds to Orai1 with sixfold symmetry

Dilshan Balasuriya, Shyam Srivats, Ruth D. Murrell-Lagnado, J. Michael Edwardson *

Department of Pharmacology, University of Cambridge, Tennis Court Road, Cambridge CB2 1PD, United Kingdom

ARTICLE INFO

Article history:
Received 24 April 2014
Revised 19 June 2014
Accepted 23 June 2014
Available online 1 July 2014

Edited by Peter Brzezinski

Keywords:
Atomic force microscopy
CRAC channel
Orai1
STIM1
Store-operated Ca^{2+} entry

ABSTRACT

Depletion of Ca^{2+} from the endoplasmic reticulum (ER) lumen triggers the opening of Ca^{2+} release-activated Ca^{2+} (CRAC) channels at the plasma membrane. CRAC channels are activated by stromal interaction molecule 1 (STIM1), an ER resident protein that senses Ca^{2+} store depletion and interacts with Orai1, the pore-forming subunit of the channel. The subunit stoichiometry of the CRAC channel is controversial. Here we provide evidence, using atomic force microscopy (AFM) imaging, that Orai1 assembles as a hexamer, and that STIM1 binds to Orai1 with sixfold symmetry. STIM1 associates with Orai1 in the form of monomers, dimers, and multimeric string-like structures that form links between the Orai1 hexamers. Our results provide new insights into the nature of the interactions between STIM1 and Orai1.

Structured summary of protein interactions:
Orai1 physically interacts with **STIM1** by anti tag coimmunoprecipitation (View interaction)
Orai1 and **STIM1** bind by atomic force microscopy (View interaction)
STIM1 and **Orai1** colocalize by fluorescence microscopy (View interaction)
STIM1 and **STIM1** bind by atomic force microscopy (1, 2)
Orai1 and **Orai1** bind by atomic force microscopy (View interaction)

1. Introduction

Depletion of Ca^{2+} within the lumen of the endoplasmic reticulum (ER) triggers Ca^{2+} influx across the plasma membrane (PM) via Ca^{2+} release-activated Ca^{2+} (CRAC) channels [1,2]. This process of store-operated Ca^{2+} entry involves two key proteins, stromal interacting molecule (STIM), an ER resident protein [3,4], and Orai, which forms the CRAC channel at the PM [5–7]. Activation of the CRAC channel occurs when STIM senses depletion of the ER Ca^{2+} store, oligomerizes and translocates to ER-PM junctions, where it binds to and activates Orai [8].

Each human Orai1 subunit has four putative transmembrane α-helices (M1–M4; [5–7]). Human STIM1 has a single transmembrane region [2], and oligomerizes in response to the release of Ca^{2+} from the EF hand domains of the extra-cytoplasmic N-terminal region [9]. The cytoplasmic C-terminal region is involved in STIM1 translocation to the ER-PM junctions and in binding to the M4 helices of Orai1 via a region called the STIM1–Orai1 activating region (SOAR) [10,11]. SOAR adopts a dimeric form [12], and upon activation of the Orai1 channel STIM1 further assembles into a higher-order oligomer using the dimer as a basic unit [13].

The CRAC channel was originally believed to consist of an Orai tetramer, based on functional analysis of Orai1 concatemers [14], gel electrophoresis [15,16], single-molecule photobleaching [17], brightness analysis [18] and high-resolution electron microscopy imaging [15]. Additionally, it was proposed that Orai1 exists as a dimer in its inactive state and then assembles into tetramers in a STIM1-dependent manner [16]. The STIM1/Orai1 stoichiometry of a functional CRAC channel complex has been suggested to be either 2:4 [17] or 8:4 [19,20].

Given the wealth of evidence for a tetrameric CRAC channel, it came as a major surprise when the crystal structure of purified *Drosophila* Orai1, along with cross-linking and size exclusion chromatography, indicated a hexameric structure [21]. This stoichiom-

Abbreviations: AFM, atomic force microscopy; CRAC, Ca^{2+} release-activated Ca^{2+} channel; ER, endoplasmic reticulum; HA, hemagglutinin; PM, plasma membrane; PAGE, polyacrylamide gel electrophoresis; STIM, stromal interaction molecule; SOAR, STIM1–Orai1 activating region

* Corresponding author. Fax: +44 1223 334100.
E-mail address: jme1000@cam.ac.uk (J.M. Edwardson).

http://dx.doi.org/10.1016/j.febslet.2014.06.054
0014-5793/

etry is still not universally accepted [22], and it has been suggested that the deletions and mutations necessary for successful crystal formation might have perturbed channel assembly.

We have developed a method, based on atomic force microscopy (AFM) imaging, for determining the stoichiometry of protein–protein interactions (e.g. [23–25]). Here, we provide evidence that full-length, wild type Orai1 assembles as a hexamer, that full-length STIM1 binds to Orai1 with sixfold symmetry, and that STIM1/Orai1 complex formation is increased by store depletion.

2. Materials and methods

2.1. Expression, solubilization and purification of proteins

tsA 201 cells were grown in Dulbecco's modified Eagle's medium supplemented with 10% (v/v) fetal bovine serum, 100 μg/ml of streptomycin and 100 units/ml of penicillin (Life Technologies, UK). Cells were grown at 37 °C, in an atmosphere of 5% CO_2/air. Human Orai1, with a C-terminal Myc/His epitope tag, and human STIM1, with an N-terminal hemagglutinin (HA) tag were expressed in the vector pcDNA3.1. Cells were transfected with DNA using the calcium phosphate method. A total of 100 μg of DNA was used to transfect 2×162 cm^3 culture flasks for single transfections of either Orai1-Myc/His or HA-STIM1. For co-transfections, 50 μg of each DNA construct was used. After transfection, cells were incubated for 48 h at 37 °C to allow protein expression. Transfected cells were either untreated or treated with 5 μM thapsigargin (Life Technologies) in the presence of 1 mM EGTA in normal extracellular solution (140 mM NaCl, 5 mM KCl, 2 mM $CaCl_2$, 1 mM $MgCl_2$, 10 mM glucose, 10 mM HEPES, pH 7.3) for 30 min at room temperature. Protein expression and intracellular localization was checked for each condition using immunofluorescence. Cells were fixed with paraformaldehyde (4% w/v), permeabilized with saponin (0.5% w/v) and incubated with appropriate antibodies: rabbit polyclonal anti-HA (Sigma, H6908) and mouse monoclonal anti-Myc (Life Technologies, R950-25), followed by fluorescein isothiocyanate-conjugated goat anti-mouse and Cy3-conjugated goat anti-rabbit (Sigma). Cells were imaged by confocal laser scanning microscopy.

Transfected cells were solubilized in 1% Triton X-100 (v/v) for 1 h at 4 °C, and the detergent extract was centrifuged at 62,000×g for 1 h to remove insoluble material. During and after solubilization, buffers contained either 2 mM Ca^{2+} (untreated) or 1 mM EGTA (thapsigargin-treated). To capture Orai1-Myc/His or HA-STIM1, the solubilized extract was incubated with anti-Myc or anti-HA agarose beads (Sigma), respectively, for 3 h. The beads were washed extensively and bound protein was eluted with Myc or HA peptide (100 μg/ml). The eluted samples were analyzed by SDS–polyacrylamide gel electrophoresis (SDS–PAGE), followed by silver staining and/or immunoblotting, using anti-Myc or anti-HA (Covance, HA.11 clone 16B12) antibodies. In one experiment, a sample containing Orai1-Myc/His was denatured and treated with N-glycosidase F (25 U/μl; New England Biolabs) for 1 h at 37 °C.

2.2. AFM imaging

Isolated proteins were diluted to ~40 pM, and 45 μl of the solution was added to a 1-cm mica disc. After 10 min, the mica was washed with water and dried under nitrogen. Samples were imaged in air using a Bruker Multimode atomic force microscope, as described previously [23–25]. The silicon cantilevers (OTESPA, Bruker) had a drive frequency of 271–321 kHz and a specified spring constant of 12–103 N/m (Mikromasch). The scan rate was 3 Hz, and the applied imaging force was kept as low as possible (target amplitude of 1.0 V and amplitude setpoint ~0.7–1.0 V).

Molecular volumes for individual STIM1 particles were determined using the Scanning Probe Image Processor Version 5 (Image Metrology). For particles within complexes, particle heights and radii were measured manually by the Nanoscope software. When proteins are dried down, they flatten on the mica substrate and adopt the shape of a spherical cap. Particle volumes were therefore calculated using the equation:

$$V_m = (\pi h/6)(3r^2 + h^2) \quad (1)$$

where h is the particle height and r is the radius [26]. Molecular volume based on molecular mass was calculated using the equation:

$$V_c = (M_0/N_0)(V_1 + dV_2) \quad (2)$$

where M_0 is the molecular mass, N_0 is Avogadro's number, V_1 and V_2 are the partial specific volumes of particle (0.74 cm^3/g) and water (1 cm^3/g), respectively, and d is the extent of protein hydration (taken as 0.4 g water/g protein). It has been shown previously that there are no significant differences in molecular volumes determined under fluid and in air [26]. Further, we [27] and others [26] have reported a very good correlation between predicted and calculated molecular volumes for proteins of widely varying molecular masses.

2.3. Analysis of binding events

AFM images were taken of complexes between Orai1 and anti-epitope antibodies, and between Orai1 and co-expressed STIM1. For antibody decoration, Orai1-Myc/His was incubated overnight with either mouse monoclonal anti-His (Life Technologies; P/N46-0693) antibody, or mouse monoclonal anti-V5 (Life Technologies; R950-25) antibody as a negative control (100 ng/ml in both cases). To be accepted for analysis, bound antibodies needed to have a molecular volume between 100 and 300 nm^3, and bound STIM1 particles needed to be larger than 100 nm^3. Volume ranges for STIM1 monomers and dimers were set at 100–200 nm^3 and 200–300 nm^3, respectively. The height of the lowest point between the peripheral and the central particle needed to be greater than 0.3 nm for the peripheral particle to be considered bound. Any particle with a length greater than twice its width was rejected. Based on the peaks of volume distributions for decorated central particles (~600 nm^3; see results) an acceptable range was set at 400–800 nm^3. To be considered a double binding event, all particles and both binding events needed to meet all the above criteria. The angles between pairs of bound antibodies and STIM1 particles were measured; a frequency distribution of angles was constructed and the angle peaks were used to deduce the stoichiometry of the complex. The angle peaks were broad, likely reflecting the fact that the complexes attach to the mica in a variety of orientations. Importantly, despite the flattening of the particles on the mica, the subunit arrangement within the central particle is faithfully reported by the geometry of the complexes (e.g. [23–25]).

2.4. Statistical analysis

Histograms were drawn with bin widths chosen according to Scott's equation:

$$\text{Bin width} = 3.5\sigma/n^{1/3} \quad (3)$$

where σ is an estimate of the standard deviation and n is the sample size [28]. Where Gaussian curves were fitted to the data, the number of curves was chosen to maximize the r^2 value while giving significantly different means using Welch's t test for unequal sample sizes and unequal variances [29].

3. Results

tsA 201 cells expressing Orai1 bearing a C-terminal Myc/His epitope tag were solubilized in Triton X-100, and protein was isolated by anti-Myc immunoaffinity chromatography. Isolated protein was analyzed by SDS–polyacrylamide gel electrophoresis (SDS–PAGE) followed by either silver staining, or immunoblotting using an anti-Myc antibody. Bands were seen at ~45 kDa and ~50 kDa on both the silver stained gel (Fig. 1A, left panel) and the immunoblot (right panel). After treatment of the protein with N-glycosidase F only a single band was seen at ~45 kDa (Fig. 1B) indicating that the two original bands represent unglycosylated and glycosylated forms of the protein.

Isolated Orai1 was imaged after incubation with an anti-His antibody, which should decorate the C terminus of each subunit. Low-magnification AFM images (Fig. 1C) revealed a population of large particles, some of which were decorated by one (arrowhead), two (arrows) or several (asterisk) smaller particles. Zoomed images of large particles in various decoration states are shown in Fig. 1D. Significantly, the angles between pairs of bound small particles were ~60°, ~120° or ~180°. We found that 26.4% (n = 70/265) of Orai1 particles were singly decorated; 7.3% (n = 32/438) were doubly decorated, 2.5% (n = 11/438) were triply decorated and 0.7% (n = 3/438) were decorated by 4–6 small particles. The extent of single and double decoration by a control (anti-V5) antibody was 3.3 and 9.7 times lower, respectively, than with the positive antibody. Further, no particles in the control were decorated by three or more small particles. Hence, the majority of decoration events represent specific binding of anti-His antibodies to Orai1 particles. A frequency distribution of volumes of decorated central particles (Fig. 1E) had a single peak at 580 ± 7 nm^3 (n = 129), very close to the expected volume for an Orai1 hexamer of molecular mass 300 kDa (570 nm^3). A frequency distribution of angles between pairs of bound antibodies (Fig. 1F) had three peaks, at 69 ± 3° (n = 40), 125 ± 5° (n = 34) and 175 ± 10° (n = 22). Angle ranges of 30–90°, 90–150° and 150–180° were set for the three

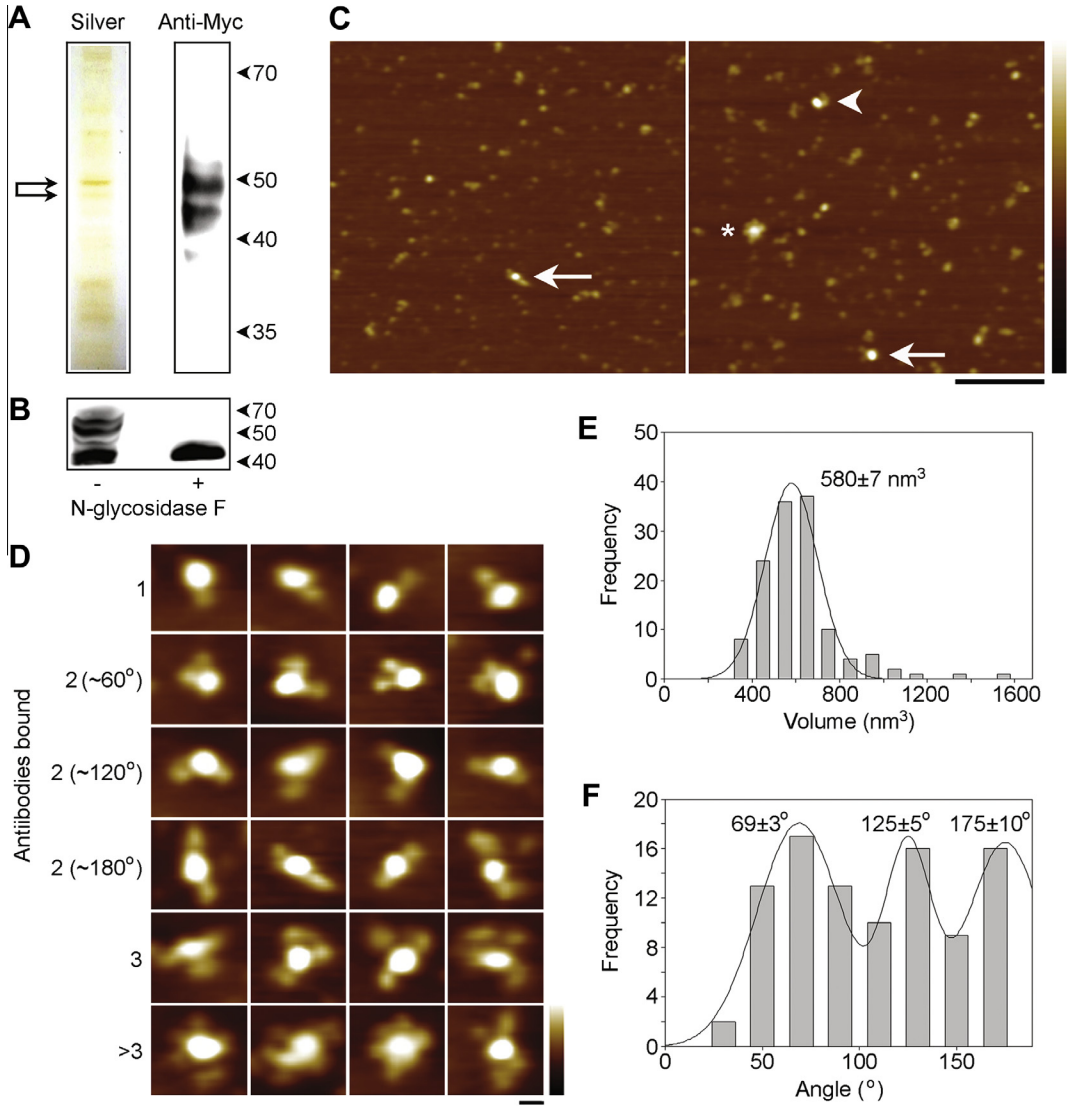

Fig. 1. Antibody decoration of Orai1 reveals a hexameric assembly state. (A) Protein was isolated from cells expressing Orai1-Myc/His by anti-Myc immunoaffinity chromatography. The silver stained gel (left panel) shows bands at ~45 and ~50 kDa (arrows). The same bands were detected on the anti-Myc immunoblot (right panel). Molecular mass markers (kDa) are shown. (B) Effect of N-glycosidase F treatment on the mobility of Orai1-Myc/His. (C) Low-magnification AFM images of Orai1 decorated by anti-His antibodies. The arrowhead (right panel) indicates a singly-decorated particle. The arrows indicate receptors doubly decorated at either ~60° (right panel) or ~180° (left panel). The asterisk (right panel) indicates a particle decorated by six antibodies. Scale bar, 200 nm; height scale, 0–4 nm. (D) Zoomed images showing antibody-decorated Orai1 particles. Scale bar, 20 nm; height scale, 0–3 nm. (E) Frequency distribution of molecular volumes of antibody-decorated Orai1 particles. The curve indicates the fitted Gaussian function. The peak of the distribution is indicated. (F) Frequency distribution of angles between pairs of bound antibodies.

peaks; the ratio of the numbers of particles within these peaks was 1.8:1.5:1. This angle profile, with three peaks at approximately 60°, 120° and 180°, in a ratio of ~2:2:1 indicates that the antibodies bind the Orai1 oligomer with sixfold symmetry, and that Orai1 therefore assembles as a hexamer, consistent with the peak molecular volume for the antibody-decorated particles.

Cells were next co-transfected with DNA encoding Orai1-Myc/His and HA-STIM1. The localization of the two proteins, with and without thapsigargin (5 μM) treatment, was determined by immunofluorescence analysis of saponin-permeabilized cells. In control cells, Orai1 was seen predominantly at the plasma membrane, whereas STIM1 was found in a reticular pattern throughout the cell cytoplasm, consistent with an ER localization (Fig. 2A). By contrast, in thapsigargin-treated cells, the STIM1 and Orai1 signals overlapped extensively, consistent with the translocation of STIM1 to sites beneath the plasma membrane [9–11]. Co-transfected cells, either untreated or thapsigargin-treated, were solubilized, and the detergent extracts were subjected to anti-Myc immunoprecipitation followed by immunoblotting with anti-Myc (Orai1) and anti-HA (STIM1) antibodies. Orai1 was present in both samples, as expected (Fig. 2B), whereas STIM1 was co-immunoprecipitated only from the extract of thapsigargin-treated cells, indicating that STIM1 associates with Orai1 only after store depletion.

A silver stained gel of protein isolated from thapsigargin-treated cells co-expressing Orai1-Myc/His and HA-STIM1 by anti-Myc immunoaffinity chromatography showed prominent bands at ~45 kDa and ~50 kDa and a fainter band at ~90 kDa (Fig. 3A, left panel). Anti-Myc and anti-HA immunoblots (Fig. 3A, right panels) confirmed that the ~45-kDa and ~50-kDa bands were Orai1, and the ~90-kDa band was STIM1. Low-magnification AFM images of the isolated sample are shown in Fig. 3B. Arrows indicate large particles decorated by two (left panel) or three (right panel) small

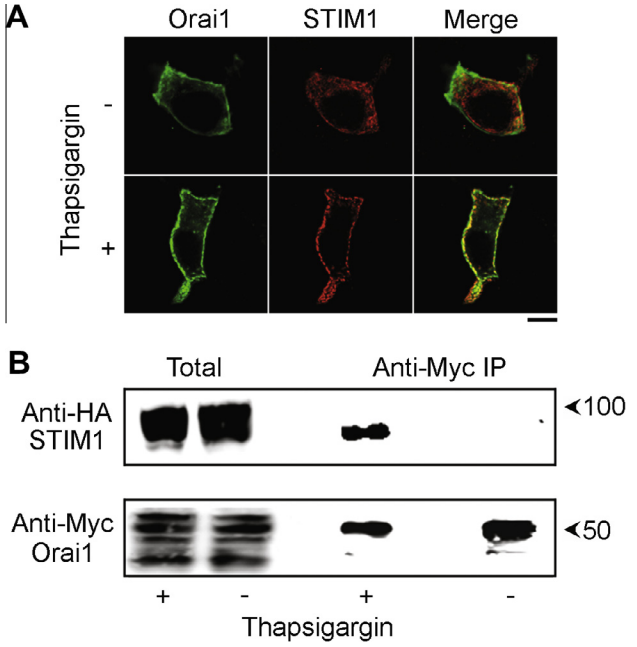

Fig. 2. STIM1–Orai1 interaction is triggered by Ca^{2+} store depletion. (A) Immunofluorescence detection of STIM1 and Orai1 in control and thapsigargin-treated (5 μM, 30 min), co-transfected cells. Cells were fixed, permeabilized and incubated with rabbit polyclonal anti-HA and mouse monoclonal anti-Myc primary antibodies, followed by fluorescein isothiocyanate-conjugated goat anti-mouse and Cy3-conjugated goat anti-rabbit secondary antibodies. Scale bar, 10 μm. (B) Co-immunoprecipitation of STIM1 and Orai1 from control and thapsigargin-treated, co-transfected cells. Protein was precipitated from clarified detergent extracts of cells using anti-Myc-agarose beads. Total extracts and immunoprecipitates were analyzed by SDS–PAGE followed by immunoblotting using anti-Myc and anti-HA antibodies.

particles. Zoomed images of large particles in various decoration states are shown in Fig. 3C. As for antibody decoration, the angles between pairs of bound small particles were ~60°, ~120° or ~180°. A frequency distribution of the volumes of all bound peripheral particles (Fig. 3D) had two peaks, at 130 ± 2 nm^3 (n = 138) and 220 ± 7 nm^3 (n = 43), representing STIM1 monomers and dimers, respectively. We used a bound particle size of >100 nm^3 to identify STIM1-decorated large particles. A frequency distribution of the decorated particles (Fig. 3E) had a single peak at 611 ± 11 nm^3 (n = 134), similar to the result for antibody-decorated Orai1 (580 nm^3) and to the expected volume of 570 nm^3 for an Orai1 hexamer. Hence, the structures shown in Fig. 3B and C are complexes between assembled Orai1 channels and STIM1. A volume range of 400–800 nm^3 was set for Orai1 channels; 16.9% (n = 71/421) of Orai1 particles were singly decorated, 5.6% (n = 36/639) were doubly decorated, and 1.4% (n = 9/639) were triply decorated with STIM1; 0.3% (n = 2/639) of the Orai1 particles had >3 bound STIM1 particles. Corresponding percentages for a control experiment with no thapsigargin treatment were as follows: 8.8% (38/431) singly decorated, 0.9% (4/431) doubly decorated and 0.2% (1/431) triply decorated. Hence, the interaction between STIM1 and Orai1 is substantially enhanced by store depletion. In another control experiment where Orai1 was expressed alone, 5.9% (n = 31/525) of Orai1 particles appeared to be singly decorated and 0.6% (n = 3/525) were doubly decorated, with no triple or multiple decoration. Hence, the majority of decoration events seen represent specific Orai1/STIM1 interactions. A frequency distribution of angles between pairs of bound STIM1 particles (Fig. 3F) had three peaks, at 70 ± 7° (n = 29), 130 ± 10° (n = 33) and 172 ± 12° (n = 15). Angle ranges of 30–90°, 90–150° and 150–180° were set for the three peaks; the ratio of the numbers of particles within each peak was 1.9:2.2:1, indicating that STIM1 binds to Orai1 with sixfold symmetry. In addition to the bound STIM1 monomers and dimers, we also saw string-like structures, likely STIM1 oligomers, bound to Orai1 particles (Fig. 3G). Rarely, these strings connected multiple Orai1-sized particles to form networks (Fig. 3H).

To further address the structure of STIM1, protein was isolated from a detergent extract of thapsigargin-treated cells expressing HA-STIM1 (without Orai1) by anti-HA immunoaffinity chromatography. A single major band was seen at ~90 kDa on both a silver stained gel (Fig. 4A, left panel) and an anti-HA immunoblot (right panel), confirming the successful isolation of the protein. A low-magnification AFM image of the isolated protein (Fig. 4B) shows single small particles, as well as doublets (arrowheads), and string-like structures (arrow) similar to those described above. Zoomed images of these two types of multimeric structures are shown in Fig. 4C. A frequency distribution of the volumes of the STIM1 particles (Fig. 4D) had two peaks, at 142 ± 3 nm^3 (n = 249) and 240 ± 7 nm^3 (n = 82), very similar to the values for the bound STIM1 particles (Fig. 3D).

4. Discussion

We show here that Orai1 particles decorated by either antibodies or STIM1 have a molecular volume consistent with a hexameric subunit stoichiometry. This result agrees with the reported crystal structure of *Drosophila* Orai1 [21], although, significantly, we have used wild type, full-length Orai1, rather than the truncated and mutated form used for crystallization. The absence of peaks representing smaller structures from the volume distribution for Orai1 isolated from quiescent cells argues against a model in which dimers, for example, are induced to assemble into functional channels in response to STIM1 binding [16]. According to the crystal structure, the Orai1 hexamer has sixfold symmetry at the level of the transmembrane regions [21]. The M4 regions (amino acids 263–301) extend into the cytoplasm, and the M4 extensions of

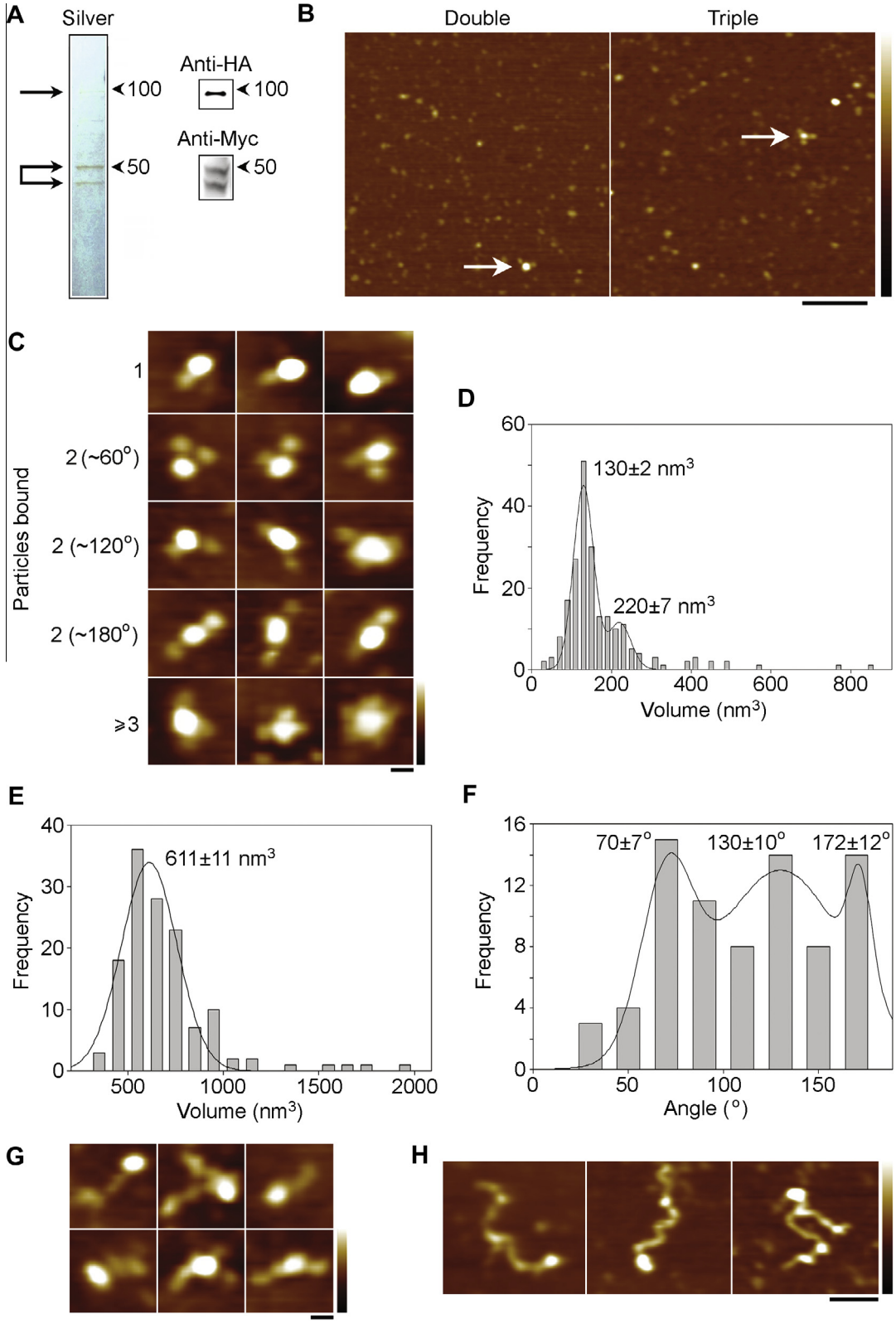

Fig. 3. STIM1 binds to Orai1 with sixfold symmetry. (A) Protein was isolated from thapsigargin-treated cells co-expressing Orai1-Myc/His and HA-STIM1 by anti-Myc immunoaffinity chromatography. The silver stained gel (left panel) shows bands at ~45, ~50 and ~90 kDa (arrows). The immunoblots (right panel) show that the ~45-kDa and ~50-kDa bands are Orai1, and the ~90-kDa band is STIM1. (B) Low-magnification AFM images of Orai1 decorated by STIM1. The arrows indicate Orai1 particles decorated by either two (left panel) or three (right panel) STIM1 particles. Scale bar, 200 nm; height scale, 0–4 nm. (C) Zoomed images showing STIM1-decorated Orai1 particles. Scale bar, 20 nm; height scale, 0–3 nm. (D) Frequency distribution of molecular volumes of bound STIM1 particles. (E) Frequency distribution of molecular volumes of STIM1-decorated Orai1 particles. (F) Frequency distribution of angles between pairs of bound STIM1 particles. (G) Zoomed images of Orai1 particles decorated by STIM1 strings. Scale bar, 20 nm; height scale, 0–3 nm. (H) Zoomed images of Orai1 particles tethered together by STIM1 strings. Scale bar, 50 nm; height scale, 0–3 nm.

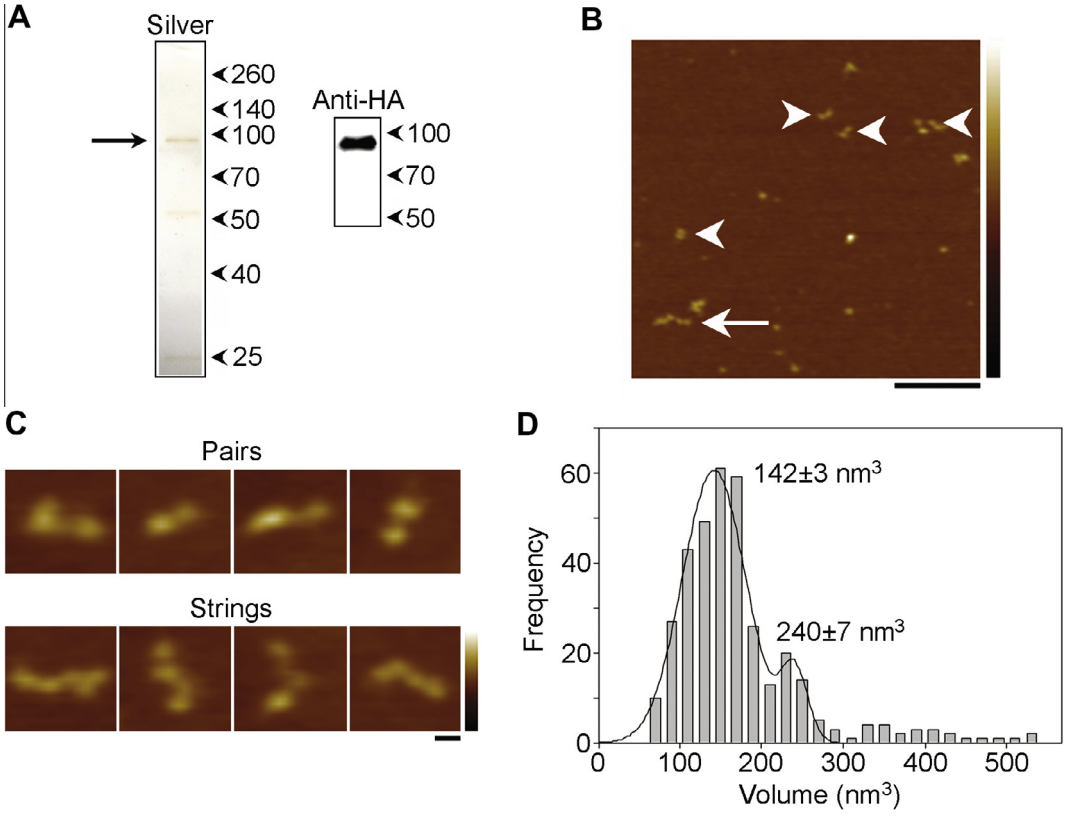

Fig. 4. STIM1 appears as monomers, dimers and string-like structures. (A) Protein was isolated from thapsigargin-treated cells expressing HA-STIM1 by anti-HA immunoaffinity chromatography. The silver stained gel (left panel) shows a major band at ~90 kDa (arrow). The same band was detected on the anti-HA immunoblot (right panel). (B) Low-magnification AFM image of STIM1. The arrowheads indicate STIM1 doublets; the arrow indicates a STIM1 string. Scale bar, 200 nm; height scale, 0–4 nm. (C) Zoomed images of STIM1 doublets (upper panels) and strings (lower panels). Scale bar, 20 nm; height scale, 0–3 nm. (D) Frequency distribution of molecular volumes of STIM1 particles.

neighboring subunits pack together in pairs, generating threefold symmetry. Consistent with this proposed architecture, a recent study based on NMR structural analysis of short C-terminal fragments of STIM1 and Orai1 indicated that a pair of Orai1 C termini binds one STIM1 dimer [30]. We suggest that the full-length proteins investigated in the present study might behave differently. For example, STIM1 binding may disrupt the interhelical hydrophobic interactions, generating sixfold binding symmetry. The sixfold symmetry of decoration of Orai1 by both antibodies and STIM1 supports the latter possibility, and suggests that antibody binding might have the same effect on the M4 helix as STIM1. In principle, the presence of the Myc/His tag at the C terminus of Orai1 may cause structural perturbation, although the crystallized protein was also tagged at its C terminus; further, it is known that the Myc/His tagged Orai1 is fully functional [7], and we have shown here that tagged Orai1 retains the ability to interact with STIM1.

Previous studies have shown that STIM1 molecules exist as dimers [13], and a crystal structure of the SOAR revealed a dimeric structure [12]. There is evidence that STIM1 is functional in this dimeric state and also interacts with Orai1 as a dimer [19]. Here, we found that STIM1 exists predominantly as monomers, both when expressed alone and when bound to Orai1, although both free and bound STIM1 also contained a significant population of dimers, which sometimes appeared in the form of doublets. It is possible that STIM1 dimers dissociate during the purification process, which might indicate a rather low-affinity interaction between the monomers. However, our results do suggest that STIM1 monomers are capable of interacting with Orai1 hexamers.

STIM1 samples also contained string-like structures that interacted with, and clustered, Orai1 hexamers. A similar clustering effect has been observed previously by negative-stain electron microscopy, using a 107-residue CRAC activating domain of STIM1 [11]. However, the string-like structures were not seen in the previous study, likely because a STIM1 fragment was used. We suggest that the STIM1/Orai1 network seen in our AFM images represent remnants of the structures that assemble within cells in response to store depletion.

In conclusion, our results reveal the hexameric assembly of full-length, wild type Orai1, and the sixfold symmetry of the STIM1/Orai1 complex.

Acknowledgements

We thank Dr. R. Penner (Honolulu) and Prof. D. Cooper (Cambridge) for providing the Orai1-Myc/His and HA-STIM1 constructs, respectively. D.B. holds a David James Bursary from the Department of Pharmacology, Cambridge. S.S. is supported by the Cambridge International and European Trust.

References

[1] Putney Jr., J.W. (1986) A model for receptor-regulated calcium entry. Cell Calcium 7, 1–12.
[2] Hogan, P.G., Lewis, R.S. and Rao, A. (2010) Molecular basis of calcium signaling in lymphocytes: STIM and ORAI. Annu. Rev. Immunol. 28, 491–533.
[3] Roos, J., DiGregorio, P.J., Yeromin, A.V., Ohlsen, K., Lioudyno, M., Zhang, S., Safrina, O., Kozak, J.A., Wagner, S.L., Cahalan, M.D., Veliçelebi, G. and Stauderman, K.A. (2005) STIM1, an essential and conserved component of store-operated Ca^{2+} channel function. J. Cell Biol. 169, 435–445.

[4] Liou, J., Kim, M.L., Heo, W.D., Jones, J.T., Myers, J.W., Ferrell Jr., J.E. and Meyer, T. (2005) STIM is a Ca^{2+} sensor essential for Ca^{2+}-store-depletion-triggered Ca^{2+} influx. Curr. Biol. 15, 1235–1241.
[5] Feske, S., Gwack, Y., Prakriya, M., Srikanth, S., Puppel, S.H., Tanasa, B., Hogan, P.G., Lewis, R.S., Daly, M. and Rao, A. (2006) A mutation in Orai1 causes immune deficiency by abrogating CRAC channel function. Nature 441, 179–185.
[6] Vig, M., Peinelt, C., Beck, A., Koomoa, D.L., Rabah, D., Koblan-Huberson, M., Kraft, S., Turner, H., Fleig, A., Penner, R. and Kinet, J.P. (2006) CRACM1 is a plasma membrane protein essential for store-operated Ca^{2+} entry. Science 312, 1220–1223.
[7] Vig, M., Beck, A., Billingsley, J.M., Lis, A., Parvez, S., Peinelt, C., Koomoa, D.L., Soboloff, J., Gill, D.L., Fleig, A., Kinet, J.P. and Penner, R. (2006) CRACM1 multimers form the ion-selective pore of the CRAC channel. Curr. Biol. 16, 2073–2079.
[8] Soboloff, J., Rothberg, B.S., Madesh, M. and Gill, D.L. (2012) STIM proteins: dynamic calcium signal transducers. Nat. Rev. Mol. Cell Biol. 13, 549–565.
[9] Stathopulos, P.B., Li, G.Y., Plevin, M.J., Ames, J.B. and Ikura, M. (2006) Stored Ca^{2+} depletion-induced oligomerization of stromal interaction molecule 1 (STIM1) via the EF-SAM region: an initiation mechanism for capacitive Ca^{2+} entry. J. Biol. Chem. 281, 35855–35862.
[10] Liou, J., Fivaz, M., Inoue, T. and Meyer, T. (2007) Live-cell imaging reveals sequential oligomerization and local plasma membrane targeting of stromal interaction molecule 1 after Ca^{2+} store depletion. Proc. Natl. Acad. Sci. U.S.A. 104, 9301–9306.
[11] Park, C.Y., Hoover, P.J., Mullins, F.M., Bachhawat, P., Covington, E.D., Raunser, S., Walz, T., Garcia, K.C., Dolmetsch, R.E. and Lewis, R.S. (2009) STIM1 clusters and activates CRAC channels via direct binding of a cytosolic domain to Orai1. Cell 136, 876–890.
[12] Yang, X., Jin, H., Cai, X., Li, S. and Shen, Y. (2012) Structural and mechanistic insights into the activation of stromal interaction molecule 1 (STIM1). Proc. Natl. Acad. Sci. U.S.A. 109, 5657–5662.
[13] Covington, E.D., Wu, M.M. and Lewis, R.S. (2010) Essential role for the CRAC activation domain in store-dependent oligomerization of STIM1. Mol. Biol. Cell 21, 1897–1907.
[14] Mignen, O., Thompson, J.L. and Shuttleworth, T.J. (2008) Orai1 subunit stoichiometry of the mammalian CRAC channel pore. J. Physiol. 586, 419–425.
[15] Maruyama, Y., Ogura, T., Mio, K., Kato, K., Kaneko, T., Kiyonaka, S., Mori, Y. and Sato, C. (2009) Tetrameric Orai1 is a teardrop-shaped molecule with a long, tapered cytoplasmic domain. J. Biol. Chem. 284, 13676–13685.
[16] Penna, A., Demuro, A., Yeromin, A.V., Zhang, S.L., Safrina, O., Parker, I. and Cahalan, M.D. (2008) The CRAC channel consists of a tetramer formed by Stim-induced dimerization of Orai dimers. Nature 456, 116–120.
[17] Ji, W., Xu, P., Li, Z., Lu, J., Liu, L., Zhan, Y., Chen, Y., Hille, B., Xu, T. and Chen, L. (2008) Functional stoichiometry of the unitary calcium-release-activated calcium channel. Proc. Natl. Acad. Sci. U.S.A. 105, 13668–13673.
[18] Madl, J., Weghuber, J., Fritsch, R., Derler, I., Fahrner, M., Frischauf, I., Lackner, B., Romanin, C. and Schütz, G.J. (2010) Resting state Orai1 diffuses as homotetramer in the plasma membrane of live mammalian cells. J. Biol. Chem. 285, 41135–41142.
[19] Li, Z., Liu, L., Deng, Y., Ji, W., Du, W., Xu, P., Chen, L. and Xu, T. (2011) Graded activation of CRAC channel by binding of different numbers of STIM1 to Orai1 subunits. Cell Res. 21, 305–315.
[20] Hoover, P.J. and Lewis, R.S. (2011) Stoichiometric requirements for trapping and gating of Ca^{2+} release-activated Ca^{2+} (CRAC) channels by stromal interaction molecule 1 (STIM1). Proc. Natl. Acad. Sci. U.S.A. 108, 13299–13304.
[21] Hou, X., Pedi, L., Diver, M.M. and Long, S.B. (2012) Crystal structure of the calcium release-activated calcium channel Orai. Science 338, 1308–1313.
[22] Thompson, J.L. and Shuttleworth, T.J. (2013) How many Orai's does it take to make a CRAC channel? Sci. Rep. 3, 1961.
[23] Barrera, N.P., Ormond, S.J., Henderson, R.M., Murrell-Lagnado, R.D. and Edwardson, J.M. (2005) AFM imaging demonstrates that $P2X_2$ receptors are trimers, but that $P2X_6$ receptor subunits do not oligomerize. J. Biol. Chem. 280, 10759–10765.
[24] Barrera, N.P., Betts, J., You, H., Henderson, R.M., Martin, I.L., Dunn, S.M.J. and Edwardson, J.M. (2008) Atomic force microscopy reveals the stoichiometry and subunit arrangement of the $\alpha_4\beta_3\delta$ $GABA_A$ receptor. Mol. Pharm. 73, 960–967.
[25] Balasuriya, D., Goetze, T.A., Barrera, N.P., Stewart, A.P., Suzuki, Y. and Edwardson, J.M. (2013) AMPA and NMDA receptors adopt different subunit arrangements. J. Biol. Chem. 288, 21987–21998.
[26] Schneider, S.W., Lärmer, J., Henderson, R.M. and Oberleithner, H. (1998) Molecular weights of individual proteins correlate with molecular volumes measured by atomic force microscopy. Pflügers Arch. 435, 362–367.
[27] Neaves, K.J., Cooper, L.P., White, J.H., Carnally, S.M., Dryden, D.T.F., Edwardson, J.M. and Henderson, R.M. (2009) Atomic force microscopy of the EcoKI type I DNA restriction enzyme bound to DNA shows enzyme dimerisation and DNA looping. Nucleic Acids Res. 37, 2053–2063.
[28] Scott, D.W. (1979) On optimal and data-based histograms. Biometrika 66, 605–610.
[29] Welch, B.L. (1947) The generalisation of student's problems when several different population variances are involved. Biometrika 34, 28–35.
[30] Stathopulos, P.B., Schindl, R., Fahrner, M., Zheng, L., Gasmi-Seabrook, G.M., Muik, M., Romanin, C. and Ikura, M. (2013) STIM1/Orai1 coiled-coil interplay in the regulation of store-operated calcium entry. Nat. Commun. 4, 2963, http://dx.doi.org/10.1038/ncomms3963.